AEM Accepts, published online ahead of print on 4 October 2013
Appl. Environ. Microbiol. doi:10.1128/AEM.02418-13
Copyright © 2013, American Society for Microbiology. All Rights Reserved.

AEM Accepts published online ahead of print

1 **Title**: Oxidation of the cyclic ethers 1,4-dioxane and tetrahydrofuran by a monooxygenase in two
2 *Pseudonocardia* species
3
4 **Running title**: Expression and Activity of a Cyclic Ether Monooxygenase
5
6 Christopher M. Sales[1,2], Ariel Grostern[2], Juanito V. Parales[3], Rebecca E. Parales[3], and Lisa
7 Alvarez-Cohen[2,4,#]
8
9 [1] Department of Civil, Architectural & Environmental Engineering, Drexel University,
10 Philadelphia, PA 19104
11 [2]Department of Civil & Environmental Engineering, University of California, Berkeley, CA
12 94720-1710
13 [3]Department of Microbiology, University of California, Davis, CA 95616
14 [4]Earth Sciences Division, Lawrence Berkeley National Laboratory, Berkeley, CA 94720
15
16 # Corresponding Author:
17 Lisa Alvarez-Cohen
18 Email: alvarez@ce.berkeley.edu
19

AEM Accepts published online ahead of print

20 **Abstract**

21 The bacterium *Pseudonocardia dioxanivorans* CB1190 grows on the cyclic ethers 1,4-dioxane
22 (dioxane) and tetrahydrofuran (THF) as sole carbon and energy sources. Prior transcriptional
23 studies indicated that an annotated THF monooxygenase (THF MO) gene cluster *thmADBC*
24 located on a plasmid in CB1190 is up-regulated during growth on dioxane. In this work,
25 transcriptional analysis demonstrates that up-regulation of *thmADBC* occurs during growth on the
26 dioxane metabolite β-hydroxyethoxyacetic acid (HEAA) and on THF. Comparison of the
27 transcriptomes of CB1190 grown on THF and succinate (an intermediate of THF degradation)
28 permitted the identification of other genes involved in THF metabolism. Dioxane and THF
29 oxidation activity of the THF MO was verified in *Rhodococcus jostii* RHA1 cells heterologously
30 expressing the CB1190 *thmADBC* gene cluster. Interestingly, these *thmADBC* expression clones
31 accumulated HEAA as a dead-end product of dioxane transformation, indicating that despite its
32 genes being transcriptionally up-regulated during growth on HEAA, the THF MO enzyme is not
33 responsible for degradation of HEAA in CB1190. Similar activities were also observed in RHA1
34 cells heterologously expressing the *thmADBC* gene cluster from *Pseudonocardia*
35 *tetrahydrofuranoxydans* K1.

36
37
38
39
40
41
42

AEM Accepts published online ahead of print

43 ## Introduction

44 Increasing evidence and awareness of the prevalence of 1,4-dioxane (dioxane) and
45 tetrahydrofuran (THF) contamination in groundwater, due mainly to their use as chlorinated
46 solvent stabilizers, has prompted research into the development of remediation strategies to
47 remove them from the environment. One strategy being investigated for treatment of these four-
48 carbon cyclic ethers is biological degradation.

49 A number of pure and mixed cultures of bacteria and fungi have been reported to degrade
50 dioxane aerobically (1-12), while only one study has reported anaerobic degradation (13). To
51 date, nine microorganisms have been reported to be capable of growth on dioxane as a sole
52 carbon and energy source (*i.e.*, metabolism of dioxane), including *Rhodococcus ruber* 219 (1),
53 *Mycobacterium* sp. PH-06 (12), *Pseudonocardia dioxanivorans* CB1190 (3, 14), *Pseudonocardia*
54 *benzenivorans* B5 (11), the fungus *Cordyceps sinensis* (9), and four recently isolated strains
55 identified as two *Mycobacterium* spp., a *Pseudonocardia* sp., and a Gram-negative *Afipia* sp.
56 (15).

57 Proposed dioxane biodegradation pathways have largely been based on detected
58 intermediates and products. The production of CO_2 from the mineralization of dioxane was
59 initially reported for CB1190 (3) and the intermediates ethylene glycol, glycolic acid, and oxalic
60 acid were subsequently detected for the fungal isolate *Cordyceps sinensis* (9). Accumulation of β-
61 hydroxyethoxyacetic acid (HEAA) was observed during co-metabolic degradation of dioxane by
62 *Pseudonocardia* sp. ENV478 initially grown on THF (10). HEAA and twelve additional
63 intermediates of dioxane degradation were subsequently detected for strain CB1190, including 2-
64 hydroxy-1,4-dioxane, 2-hydroxyethoxyacetaldehyde, 1,4-dioxane-2-one, 1,3-
65 dihydroxyethoxyacetic acid, 2-hydroxyethoxy-2-hydroxyacetic acid, glycoaldehyde, glyoxal, and

AEM Accepts published online ahead of print

66 formic acid (16). Even though a dioxane degradation pathway was proposed based on these
67 detected intermediates (16), genes likely associated with several enzymatic steps in the pathway
68 were only recently identified (17). Transcriptional analyses showed that the putative THF
69 monooxygenase (MO) gene cluster *thmADBC* in strain CB1190 was the only MO out of eight
70 previously identified by genome sequencing (18) that was up-regulated during growth on dioxane
71 versus glycolate. However, unclear from this analysis was whether *thmADBC* is involved only in
72 the oxidation of dioxane or if it is also responsible for the oxidation of HEAA, as proposed by
73 Mahendra *et al.* (16).

74 Metabolism of THF has also been reported in nine bacterial strains, including *Rhodococcus*
75 *ruber* strains 219 (1), M2 (19), and ENV425 (10), a variety of *Pseudonocardia* strains, including
76 CB1190 (3), B5 (11), and ENV478 (10), *Pseudonocardia sulfidooxydans* (20) and
77 *Pseudonocardia tetrahydrofuranoxydans* K1 (21, 22). In addition, three fungal isolates are
78 capable of growth on THF, including *Cordyceps sinensis* (9), *Aureobasidium pullulans* (5), and
79 *Graphium* sp. ATCC 58400 (7). Biochemical evidence from a number of studies indicates that
80 the initial step in the aerobic biodegradation of THF, as with dioxane, is catalyzed by a MO
81 reaction. Common among proposed metabolic pathways for THF degradation for *R. ruber*
82 219 (1), *P. tetrahydrofuranoxydans* K1 (22), and *Graphium* sp. (7) is the initial oxidation of THF
83 to 2-hydroxytetrahydrofuran and the formation of succinate as a downstream intermediate. The
84 four-subunit THF MO gene cluster (*thmADBC*) from strain K1 was cloned and sequenced, and
85 transcriptionally implicated in the oxidation of THF to 2-hydroxytetrahydrofuran (22). In
86 addition to CB1190 and K1, homologs of the *thm* cluster have been found in *Pseudonocardia*
87 strain ENV478 (10, 23) and *Rhodococcus* sp. YYL (24). In the fungus *Graphium* sp. ATCC

AEM Accepts published online ahead of print

88 58400, a cytochrome P450 MO enzyme was suggested to catalyze the initial oxidation of
89 THF (7).

90 In this study, the function of the THF MO in the degradation of dioxane and THF was
91 examined. Transcriptomic microarray data from CB1190 grown on dioxane and THF and their
92 respective intermediates were analyzed to identify differentially expressed genes involved in the
93 metabolism of these cyclic ethers. Additionally, functionally active heterologous clones
94 expressing the genes *thmADBC* from strains CB1190 and K1 were constructed and used to
95 demonstrate the functional role of THF MO in the oxidation of dioxane and THF. The
96 identification and functional characterization of THF MO will enable more effective detection
97 and quantification of this important enzyme in the environment, leading to improved
98 understanding of the fate and potential for bioremediation of cyclic ethers in the field.

99 Methods

100 **Laboratory strains and culture conditions.** The bacterial strains used in this study were *P.*
101 *dioxanivorans* CB1190 (3, 14), *P. tetrahydrofuranoxydans* K1 (20), *Rhodococcus jostii*
102 RHA1 (25), and electrocompetent *Escherichia coli* DH5α (New England Biolabs, Ipswich, MA).
103 CB1190 cells were grown in ammonium mineral salts (AMS) liquid medium (3). The growth
104 substrates dioxane, THF, succinate, glycolate, isopropanol, pyruvate, and glucose were added to
105 the culture medium to achieve a final concentration of 5 mM, while HEAA was added to cultures
106 at a final concentration of 1.5 mM. The potassium salt of HEAA was prepared by CanSyn
107 Chemical Corporation (Toronto, ON). Cultures were incubated aerobically, while shaking at 150
108 rpm at 30 ºC.

109 **Cell harvesting and RNA extraction for transcriptional studies.** CB1190 cells were harvested
110 for transcriptomic microarray analysis, reverse transcriptase PCR (RT-PCR), and quantitative

AEM Accepts published online ahead of print

111 RT-PCR (qRT-PCR) using the methods described in Grostern *et al.* (17). Briefly, cells from
112 replicate bottles were collected by filtration onto 0.22 µm PVDF Durapore membrane filters
113 (Millipore, Billerica, MA). The cells from each filter were scraped with a sterile scalpel, and
114 transferred to 2 mL screw-top microcentrifuge tubes containing 1 gram of 100-µm-diameter
115 zirconia-silica beads (Biospec Products, Bartlesville, OK). Harvested cells were stored at -80ºC
116 until total nucleic acids extraction.

117 Nucleic acids were extracted using a modified version of the phenol method described
118 previously (26). Briefly, each 2 mL microcentrifuge tube containing cells and zirconia-silica
119 beads was filled with 250 µL lysis buffer (50 mM sodium acetate, 10 mM EDTA [pH 5.1]), 100
120 µL 10% sodium dodecyl sulfate, and 1.0 mL phenol (pH 8; Sigma Aldrich, St. Louis, MO). Cells
121 were lysed by heating to 65ºC for 2 min, bead beating with a Mini Bead Beater (Biospec
122 Products) for 2 min, incubating at 65ºC for 8 min, and bead beating for an additional 2 min.
123 Cellular debris was collected by centrifugation (5 min at 14,000 x *g*), and the aqueous lysate was
124 transferred to new microcentrifuge tubes. The lysate was extracted twice with one volume of
125 phenol-chloroform-isoamyl alcohol (pH 8) (24:24:1, vol/vol) and once with 1 volume of
126 chloroform-isoamyl alcohol (24:1, vol/vol). Nucleic acids were precipitated with 0.1 volumes of
127 3 M sodium acetate and one volume of ice-cold isopropanol, followed by incubation at -20ºC
128 overnight. The precipitate was collected by centrifugation (30 min at 21,000 x *g* at 4 ºC), washed
129 once with 70% ethanol, and re-suspended in 100 µL nuclease-free water.

130 To obtain RNA, re-suspended nucleic acids were initially separated with the AllPrep kit
131 (Qiagen, Valencia, CA), and then the RNA was purified using the RNeasy kit (Qiagen).
132 Following elution with 100 µL RNase-free water, RNA was subjected to DNase I treatments
133 using the DNA-free kit (Ambion, Carlsbad, CA), according to the manufacturer's instructions,
134 until all contaminating DNA was removed (*i.e.,* when qPCR analysis showed C_T value > 35).

AEM Accepts published online ahead of print

135 DNase-treated RNA was subjected to a final clean-up using an RNeasy kit before performing
136 gene expression analyses.

137 **Analytical techniques.** Dioxane and THF concentrations were monitored by gas
138 chromatography with a Varian 3400 GC equipped with a flame ionization detector (FID), as
139 described previously (11). The production and degradation of HEAA was measured by liquid
140 chromatography tandem mass spectrometry (LC-MS/MS) using a hydrophilic interaction
141 chromatography (HILIC) column. Culture samples were filtered before analysis, using 0.2 µm
142 syringe filters to remove cells. Standards and samples were measured on an Agilent Technologies
143 1200 Series LC system equipped with an Agilent Technologies Zorbax HILIC Plus column (4.6
144 mm x 100 mm, 3.5 µm) coupled to an Agilent Technologies 6410 tandem triple quadrupole
145 (QQQ) mass spectrometer (Santa Clara, CA). The LC solvents used were Solvent A: aqueous
146 buffer and Solvent B: acetonitrile. The aqueous buffer was composed of 10 mM ammonium
147 formate in water with formic acid to adjust acidity (pH 5), filtered through a 0.45 µm filter. The
148 flow rate was 0.5 mL/min. The gradient was: t = 0 min, 95% B; t = 10 min, 40% B; t = 13 min,
149 95% B; t = 15 min, 95% B. The injection volume for samples and standards was 10 µL. Column
150 effluent was introduced into the electrospray chamber, where the electrospray ionization was set
151 to 3000 V in negative mode (ESI-). Nitrogen was used as the nebulizing gas at 30 psi, 325ºC, and
152 a gas flow of 11 L/min. Multiple reaction monitoring (MRM) was used to monitor the transitions
153 from the parent ion of HEAA, *m/z* 119 $[C_4H_7O_4]^-$ to the major product ions of *m/z* 119 $[C_4H_7O_4]^-$,
154 *m/z* 101 $[C_4H_5O_2]^-$, *m/z* 75 $[C_2H_3O_3]^-$, and *m/z* 31 $[CH_3O]^-$. The collision gas used for MRM was
155 argon, with the collision energy of 6 V and a fragmentor voltage of 70 V for all MRM transitions.
156 The summation of the peak areas for all MRM transitions was used for quantification of
157 standards and samples.

AEM Accepts published online ahead of print

158 **Microarray studies.** Transcriptomic microarray hybridization and imaging was performed on
159 custom Affymetrix GeneChips (Santa Clara, CA) as previously described (17). All microarray
160 data analyses were performed in the R statistical programming environment (www.r-project.org)
161 using packages available from Bioconductor version 2.9 (www.bioconductor.org) (27).
162 Hybridization signal intensities for probe sets were calculated using the "rma" function from the
163 "affy" package (28). Identification of differentially expressed genes was accomplished using the
164 "limma" package (29). Comparisons were made between groups of arrays in a contrast matrix,
165 including all treatments (dioxane, glycolate, THF, and succinate) compared to the control
166 (pyruvate) or direct comparison between treatments (*e.g.*, dioxane to glycolate or THF to
167 succinate). Each biological triplicate for all growth conditions (THF and succinate in this study;
168 dioxane, glyoclate, and pyruvate in Grostern *et al*. (17)) was analyzed on a single microarray.
169 Contrast matrices were applied to the linear fitted microarray data using the function
170 "contrast.fit". Estimated log-fold changes ($\log_2$FC) and differential expression statistics between
171 contrasts were determined using an empirical Bayes method and *P* values from linear modeling
172 were adjusted to correct for multiple hypothesis testing using the Benajamini and Hochberg
173 procedure (30) with a false discovery rate (FDR) of 1% and a $\log_2\text{FC} \geq |1|$.

174 **RT-PCR and RT-qPCR analyses.** For RT-qPCR transcriptional analyses, CB1190 was initially
175 grown on 5 mM of glucose in AMS medium and harvested by filtration. The harvested cells were
176 washed and re-suspended in AMS medium to remove glucose. Each exposure treatment (dioxane,
177 THF, and propane) and control (glucose) condition was tested in triplicate. Total RNA was
178 isolated from cells after 8 h of exposure to either 5 mM of dioxane, 5 mM of THF, 20% (vol/vol
179 of total headspace) of propane, or 5 mM of glucose (control). The isolated RNA was used to
180 synthesize cDNA using the TaqMan reverse transcription kit (Applied Biosystems, Foster City,

AEM Accepts published online ahead of print

181 CA). TaqMan chemistry was used for qPCR reactions targeting *thmA* (Psed_6976), *prmA*
182 (Psed_0639), *tpi* (Psed_3417), *thiC* (Psed_6168), and *rpoD* (Psed_0376). The genes *tpi*, *thiC*, and
183 *rpoD* were determined by the geNorm method (31) to be stably transcribed across all treatments,
184 and were thus used as internal references. qPCR reactions were performed in triplicate for each
185 biological replicate on an Applied Biosystems StepOne Plus real-time PCR system and consisted
186 of 1X Fast Universal Mix (Applied Biosystems), 2 μL of cDNA, each primer at 0.5 mM, and the
187 probe at 145 nM. The cycling conditions were: 95 ºC for 20 s, then 40 cycles of 95ºC for 1 s
188 followed by annealing for 20 s at 60 ºC. The efficiency of each qPCR assay was determined with
189 a serial dilution of cDNA derived from a dioxane treatment replicate. Gene expression was
190 normalized using the method of Vandesompele *et al.* (31).

191 Cells for RT-PCR analysis of the *thmADBC* genes were grown on dioxane, isopropanol, or
192 THF and harvested by centrifugation. RNA was isolated using the RNeasy kit. RT-PCR was
193 performed using the Qiagen One Step RT-PCR kit. The primers used for amplification of each
194 fragment can be found in Table S1 in Supplementary Material.

195 **Cloning and heterologous expression of THF MO genes in RHA1.** A 4.3 Kb fragment
196 corresponding to CB1190 genes Psed_6976-6979 was inserted into plasmid pK18 (32), and then
197 subcloned into plasmid pTip-QC2 (33), which was named pTip-CB110-thfmo. A detailed
198 description of cloning procedures and the growth of RHA1 expressing *Pseudonocardia* THF MO
199 can be found in Supplementary Materials and Methods. Cloning of the *thmADBC* gene cluster
200 from *P. tetrahydrofuranoxydans* K1 was done similarly to above, except the gene cluster was
201 amplified directly from K1 gDNA and digested, along with vector pTip-QC1, using EcoRI and
202 NcoI prior to ligation.

203 To perform oxidation assays, frozen aliquots of RHA1(pTip-CB1190-thfmo), RHA1(pTip-
204 K1-thfmo) and RHA1(pTip-QC2) were thawed and re-suspended in 1 mL of cold phosphate

AEM Accepts published online ahead of print

205 buffer. The transformation of dioxane and THF and the production of HEAA were tested in
206 triplicate in 2 mL microcentrifuge tubes containing 900 µL of buffer and a 100 µL cell
207 suspension. Each triplicate tube was amended with dioxane (2.5 mM) or THF (4.0 mM) from
208 aqueous stocks. Buffer controls (no cells) were prepared in parallel. Tubes were incubated at
209 30ºC with horizontal shaking at 150 rpm. At several time points, 200 µL samples were removed
210 and analyzed for the disappearance of the amended compound, using GC-FID (for dioxane and
211 THF) and LC-MS/MS (for HEAA).

212 **MO acetylene inhibition assays.** CB1190 was grown on dioxane (10 mM) in AMS medium,
213 cells were harvested by 0.22 µm filtration and filters were washed with 20 mM phosphate buffer
214 (pH 7) to remove residual dioxane. 5 mg (wet weight) of cells were aliquoted into eight serum
215 vials (10 mL, Bellco, Vineland NJ), the cells were resuspended in 2 mL of phosphate buffer
216 (20mM), and the vials sealed with black butyl rubber stoppers. 25% (vol/vol) acetylene was
217 added to the headspace of half of the vials, and all vials were incubated for 45 min at 30 ºC with
218 shaking at 150 rpm. Acetylene was then removed by bubbling all vials with N_2 for 5 min.
219 Dioxane (0.57 mM) or HEAA (0.57 mM) was added to two sets (acetylene-treated and non-
220 acetylene treated) of duplicate vials, and sodium formate (20 mM) was added to all vials as an
221 external energy source. Duplicate no-cell controls were prepared in parallel. The vials were
222 incubated at 30ºC with horizontal shaking at 150 rpm. The concentration of dioxane and HEAA
223 in acetylene-exposed, non-acetylene-exposed, and abiotic controls was monitored over time.

224 **Microarray data accession numbers.** Details of the experimental design and data for the
225 transcriptomic analysis of THF- and succinate-grown strain CB1190 have been deposited in the
226 NCBI Gene Expression Omnibus (GEO; http://www.ncbi.nlm.nih.gov/geo/) and are accessible
227 through GEO Series accession number GSE48814. The CEL files containing the raw

AEM Accepts published online ahead of print

228 transcriptomic data for dioxane-, glycolate-, and pyruvate-grown CB1190 were submitted for a
229 previous study (17) under the GEO Series accession number GSE33197.

230 ## Results and Discussion

231 **Differential gene expression during growth on THF, succinate, and pyruvate.** A proposed
232 reaction pathway for aerobic THF metabolism in CB1190 (Fig. 1), based on differential gene
233 expression analysis of CB1190 grown on THF, succinate, and pyruvate, has been adapted from
234 the pathways proposed by Bernhardt and Diekmann (1), Skinner *et al.* (7), and Thiemer *et*
235 *al.* (22). Succinate was chosen as a growth substrate for differential gene expression analysis
236 because it was previously identified as an intermediate of THF biodegradation in the bacterium
237 *P. tetrahydrofuranoxydans* K1 (22), as well as in the fungus *Graphium* sp. ATCC 58400 (7).
238 Transcriptomic microarray results showed that a total of 796 genes were differentially expressed
239 when CB1190 was grown on THF versus succinate, with 210 up-regulated and 586 down-
240 regulated (Table S3). Relative to previously collected transcriptomics data of pyruvate-grown
241 CB1190 (17), 669 and 553 genes were differentially expressed on THF and succinate,
242 respectively (Tables S4 and S5), with 220 up-regulated on THF and 366 up-regulated on
243 succinate.

244 Among the genes up-regulated on THF but not succinate, relative to pyruvate (Table 1 and
245 Table S2), is the annotated THF MO gene cluster, *thmDBC*, Psed_6977- Psed_6979, located on
246 plasmid pPSED02. In strain K1, *thmADBC* is thought to be involved in the hydroxylation of THF
247 to 2-hydroxytetrahydrofuran, since Northern Blot analysis showed the *thm* cluster being
248 transcribed during THF utilization (22). Although the CB1190 microarray used in this current
249 study lacks a probe set for the gene encoding the α-subunit (*thmA*), RT-qPCR demonstrated that
250 short-term (8 h) exposure of CB1190 cells to THF leads to up-regulation of *thmA* transcription by

AEM Accepts published online ahead of print

251 10-fold when compared to unexposed cells. Short-term exposure to dioxane or propane was also
252 shown to induce *thmA* expression by 24-fold and 6-fold, respectively. The gene expression of the
253 α-subunit (*thmA*) was chosen for qPCR analysis because the α-subunit of the propane
254 monooxygenase encoding the large hydroxylase component in *R. jostii* RHA1 was previously
255 found to be the most highly expressed gene in its *prmABCD* cluster (34). Furthermore, RT-PCR
256 of the putative THF MO genes *thmADBC* indicated that all of the genes in this cluster were co-
257 transcribed during growth on THF (Fig. S1). In addition to *thmADBC*, genes encoding an alcohol
258 dehydrogenase GroES domain protein (Psed_0131), an aldehyde dehydrogenase (*aldH*,
259 Psed_6981), and a Mn^2+/Fe^2+ transporter (Psed_6982) were also up-regulated in the presence of
260 THF relative to both succinate and pyruvate (Table 1). While the conversion of 2-
261 hydroxytetrahydrofuran to γ-butyrolactone had been proposed to be catalyzed by an alcohol
262 dehydrogenase (7), our results provide transcriptional evidence for the involvement of a specific
263 alcohol dehydrogenase in THF degradation.

264 Following abiotic hydrolysis of γ-butyrolactone to 4-hydroxybutyrate, the next enzymatic
265 reaction in the THF degradation pathway is the transformation of 4-hydroxybutyrate to succinic
266 semialdehyde, potentially catalyzed by a hydroxyacid-oxoacid transhydrogenase (35) or a 4-
267 hydroxybutyrate dehydrogenase (36). According to the transcriptomic results, two genes
268 (Psed_6970 and Psed_6971) located just upstream of the thm cluster on plasmid pPSED02 were
269 up-regulated in the presence of THF but not with succinate, relative to pyruvate (Table 1).
270 Psed_6970 encodes for a lactate dehydrogenase, a homolog of 4-hydroxybutyrate dehydrogenase,
271 which has been reported to convert 4-hydroxybutyrate to succinic semialdehyde using NAD (37),
272 while Psed_6971 encodes a hydroxyacid-oxoacid transhydrogenase. Also up-regulated in the *thm*
273 gene cluster on plasmid pPSED02 was the succinate semialdehyde dehydrogenase encoding gene

AEM Accepts published online ahead of print

274 *sad* (Psed_6975; Table 1), whose product is predicted to catalyze the next transformation step,
275 oxidation of succinate semialdehyde to succinate (22).

276 Although the proposed pathway for THF metabolism in CB1190 based upon gene expression
277 analyses (Fig. 1) shares many similarities with those proposed for *P. tetrahydrofuranoxydans*
278 K1 (22) and *Graphium* sp. ATCC 58400 (7), one notable difference between the CB1190 and K1
279 pathways is the biochemical evidence for the tautomeric transformation of 2-
280 hydrotetrahydrofuran to 4-hydroxybutyraldehyde in CB1190, similar to that proposed in the
281 fungus. The exclusion of this transformation step in the THF pathway in strain K1 was based on
282 transcriptional results indicating that *aldH* was not expressed during growth on THF (22).
283 However, *aldH* on pPSED02 near the *thm* cluster in CB1190 (Psed_6981) was up-regulated
284 during growth on THF, suggesting that tautomeric conversion of 2-hydroxytetrahydrofuran likely
285 occurs during THF degradation, as proposed in Fig. 1.

286 **The protein product of *thmADBC* oxidizes dioxane and THF.** In order to verify the THF and
287 dioxane transformation activity of the enzyme encoded by *thmADBC,* the gene cluster from
288 CB1190 was inserted into pTip-QC2 and used to transform *R. jostii* RHA1. RHA1 was chosen as
289 a host for expression of *thmADBC* for several reasons: (1) it belongs to the same *Actinomycetales*
290 order as CB1190 (25), (2) its wild-type is unable to oxidize or otherwise transform dioxane or
291 THF (data not shown), and (3) it expresses an analogous multicomponent propane
292 monooxygenase *prmABCD* (34), which has a similar GC-content (64%) as *thmADBC* of CB1190
293 (60%). Whole cells of RHA1(pTip-CB1190-thfmo), following growth on nutrient broth and
294 induction by thiostrepton, demonstrated nearly complete transformation of 4 mM THF within 3
295 days (Fig. 2A). The amount of THF loss in the abiotic and RHA1(pTip-QC2) controls was
296 minimal and could be attributed to the volatility of THF [Henry's constant $H_c = 7.05 \times 10^{-3}$ atm-

AEM Accepts published online ahead of print

297 m^3/mol] (38). RHA1(pTip-CB1190-thfmo) suspensions degraded 2.5 mM dioxane within 3 days
298 (Fig. 2B), while dioxane loss in the abiotic and RHA1(pTip-QC2) controls were negligible. The
299 dioxane degradation pathway intermediate HEAA accumulated stoichiometrically with dioxane
300 disappearance. No dioxane transformation activity was detected in cell-free extracts prepared by
301 bead-beating or sonication of RHA1(pTip-CB1190-thfmo) cells, even with the addition of the
302 MO electron donor NADH.

303 The *thmADBC* gene cluster was also cloned from *P. tetrahydrofuranoxydans* K1 and
304 expressed in RHA1 cells using the pTip-QC1 vector (RHA1(pTip-K1-thfmo)). As with
305 RHA1(pTip-CB1190-thfmo), RHA1(pTip-K1-thfmo) transformed both THF and dioxane (Fig.
306 S2), and HEAA was produced in stoichiometric amounts from dioxane (data not shown).
307 RHA1(pTip-K1-thfmo) and RHA1(pTip-CB1190-thfmo) removed nearly equivalent (~1 mM)
308 amounts of dioxane and THF over 77 h (Fig. S2).

309 The demonstration of THF and dioxane oxidation activity in the two RHA1 clones is
310 significant for two reasons: (1) it confirms the role of the CB1190 THF MO in the initial
311 oxidation of these two cyclic ethers, and (2) it demonstrates that RHA1 can be used as a
312 heterologous host for expression of multi-component MOs. In addition to this study, functional
313 genetic evidence for the involvement of THF MO genes (*thm*) has been demonstrated in
314 *Pseudonocardia* sp. strain ENV478, in which decreased translation of the *thmB* gene, caused by
315 antisense RNA, resulted in loss of its ability to degrade THF and oxidize 1,4-dioxane (23). To
316 date, we have been unable to express active THF MO from CB1190 in *E. coli*, as well as active
317 propane MO enzymes encoded by the *prmABCD* gene clusters from the actinomycetes RHA1
318 (39) and *Gordonia* sp. TY-5 (40). In support of our finding that the expression of multi-
319 component MOs is easier in actinomycete hosts, a recent study by Furuya *et al.* (41) reported the

AEM Accepts published online ahead of print

320 heterologous expression of *mimABCD* gene clusters from *Mycobacterium smegmatis* strain
321 mc^{2}155 and *Mycobacterium goodii* strain 12523. These gene clusters encode for binuclear
322 monooxygenases involved in the oxidization of propane and phenol in the host *Rhodococcus*
323 *opacus* B-4.

324 **HEAA induces, but is not transformed by, the CB1190 THFMO.** It was previously proposed
325 that the MO enzyme that catalyzes the first oxidation step in the dioxane degradation pathway
326 may also hydroxylate HEAA, leading to the formation of a number of 2-carbon intermediates
327 (16). Our previous transcriptomic study showed that the *thm* gene cluster was the only MO-
328 encoding cluster of CB1190 to be up-regulated during growth on dioxane (17). However, those
329 transcriptomic results did not clarify whether the same MO catalyzes the hydroxylation of both
330 dioxane and HEAA, necessitating additional functional studies to clarify the nature of HEAA
331 transformation in CB1190.

332 HEAA supported the growth of CB1190, with complete removal of 1.5 mM HEAA within 11
333 days by a culture inoculated with a 1:500 dilution of dioxane-grown cells (Fig. 3A). RT-qPCR
334 analysis was used to compare the transcriptional level of *thmA* in HEAA- and pyruvate-grown
335 cells. Normalized to the housekeeping genes *tpi* (Psed_3417) and *rpoD* (Psed_3051), *thmA* was
336 transcribed 41-fold higher in HEAA-grown cells than in pyruvate-grown cells. We previously
337 showed that dioxane, but not the dioxane degradation metabolite glycolate, induced *thmA* 15-fold
338 relative to pyruvate (17). Although gene expression results appear to indicate that the THF MO is
339 involved in HEAA transformation, the accumulation of HEAA in RHA1(pTip-CB1190-thfmo)
340 clones degrading dioxane (Fig. S2B) demonstrates the inability of the THF MO to degrade
341 HEAA.

342 In addition to the RHA1(pTip-CB1190-thfmo) clones, the RHA1(pTip-K1-thfmo) clones also
343 demonstrated HEAA generation and accumulation when exposed to dioxane (Fig. 2B and S2).

AEM Accepts published online ahead of print

344 Even after prolonged incubation (48 h), these clones were not able to degrade HEAA (data not
345 shown). These results support the hypothesis that the THF MO encoded by the *thmADBC* gene
346 cluster is not responsible for the transformation of HEAA.

347 Brief exposure of acetylene gas can cause irreversible inhibition of specific types of MO
348 enzyme activity (42-46) and may specifically inhibit the oxidation of dioxane (11, 16). In order to
349 test the hypothesis that an acetylene-sensitive MO is involved in the transformation of HEAA by
350 CB1190 (16), resting cells of dioxane-grown CB1190 were exposed to acetylene and then
351 dioxane and HEAA degradation were monitored. During the first couple of hours, cells pre-
352 exposed to acetylene removed negligible dioxane (Fig. 3B), but degraded 0.5 mM HEAA (Fig.
353 3C), which was similar to the positive control (cells not exposed to acetylene). After two hours,
354 some dioxane removal was observed in acetylene-exposed cells, likely due to *de novo* THF MO
355 synthesis. These results contradict the hypothesis that an acetylene-sensitive MO enzyme is
356 responsible for HEAA degradation. Further, we had previously observed that HEAA is a
357 transient metabolite generated during dioxane degradation, appearing and disappearing within a
358 short span of time (1-4 hr) rather than accumulating while dioxane is still detectable (16).
359 Together with the data in figures 2B and 3C, this indicates that dioxane and HEAA
360 transformations are performed simultaneously rather than step-wise by CB1190, supporting the
361 hypothesis that two different enzymes are responsible for the two oxidation reactions.

362 **Potential alternative mechanisms for HEAA transformation in CB1190.** The *thm* gene cluster
363 is present in CB1190 (18), K1 (22) and ENV478 (18, 22, 23). Heterologous expression
364 demonstrated that in both CB1190 and K1, this gene cluster encodes a monooxygenase that
365 transforms both THF and dioxane, while similar activity for this gene cluster was suggested by
366 gene knockdown techniques in ENV478 (23). Unlike CB1190, K1 and ENV478 degrade dioxane
367 co-metabolically. However, ENV478 accumulates HEAA as a dead-end product of dioxane

AEM Accepts published online ahead of print

368 degradation (10) while K1 does not accumulate HEAA (16). Thus, it is plausible that CB1190
369 and K1 both express enzymes that catalyze the transformation of HEAA that ENV478 lacks.
370 Given K1's ability to mineralize dioxane (16), its inability to metabolize dioxane for supporting
371 growth remains unresolved.

372 In addition to MOs, a variety of non-MO enzymes have been reported to catalyze ether bond
373 cleavage, including dioxygenases, ether hydrolases, carbon-oxygen lyases, peroxidases, laccases,
374 and etherases (47). Further studies with CB1190, K1, and other strains capable of growth on
375 dioxane are needed to identify the enzymes involved in HEAA transformation during dioxane
376 biodegradation.

377 Acknowledgements

378 This project was funded by the Strategic Environmental Research and Development Program
379 (SERDP ER-1417) and NIEHS Superfund Basic Research Program grant ES04705-19. Plasmids
380 pTip-QC2 and pTip-QC1 were obtained from the National Institute of Advanced Industrial
381 Science and Technology (Japan).

382 References

383 1. **Bernhardt D, Diekmann H.** 1991. Degradation of dioxane, tetrahydrofuran and other
384 cyclic ethers by an environmental *Rhodococcus* strain. Appl Microbiol Biotechnol
385 **36:**120-123.
386 2. **Burback BL, Perry JJ.** 1993. Biodegradation and biotransformation of groundwater
387 pollutant mixtures by *Mycobacterium vaccae*. Appl Environ Microbiol **59:**1025-1029.
388 3. **Parales RE, Adamus JE, White N, May HD.** 1994. Degradation of 1,4-dioxane by an
389 actinomycete in pure culture. Appl Environ Microbiol **60:**4527-4530.
390 4. **Roy D, Anagnostu G, Chaphalkar P.** 1994. Biodegradation of dioxane and diglyme in
391 industrial waste. J Environ Sci Health A Tox Hazard Subst Environ Eng **29:**129.
392 5. **Patt TE, Abebe HM.** 1995. Microbial degradation of chemical pollutants. USA patent
393 5399495.
394 6. **Raj CBC, Ramkumar N, Siraj AHJ, Chidambaram S.** 1997. Biodegradation of acetic,
395 benzoic, isophthalic, toluic and terephthalic acids using a mixed culture: Effluents of PTA
396 production. Proc Saf Environ **75:**245-256.

AEM Accepts published online ahead of print

397 7. **Skinner K, Cuiffetti L, Hyman M.** 2009. Metabolism and cometabolism of cyclic ethers
398 by a filamentous fungus, a *Graphium* sp. Appl Environ Microbiol **75:**5514-5522.
399 8. **Zenker MJ, Borden RC, Barlaz MA.** 2000. Mineralization of 1,4-dioxane in the
400 presence of a structural analog. Biodegradation **11:**239-246.
401 9. **Nakamiya K, Hashimoto S, Ito H, Edmonds JS, Morita M.** 2005. Degradation of 1,4-
402 dioxane and cyclic ethers by an isolated fungus. Appl Environ Microbiol **71:**1254-1258.
403 10. **Vainberg S, McClay K, Masuda H, Root D, Condee C, Zylstra GJ, Steffan RJ.** 2006.
404 Biodegradation of ether pollutants by *Pseudonocardia* sp strain ENV478. Appl Environ
405 Microbiol **72:**5218-5224.
406 11. **Mahendra S, Alvarez-Cohen L.** 2006. Kinetics of 1,4-dioxane biodegradation by
407 monooxygenase-expressing bacteria. Environ Sci Technol **40:**5435-5442.
408 12. **Kim YM, Jeon JR, Murugesan K, Kim EJ, Chang YS.** 2009. Biodegradation of 1,4-
409 dioxane and transformation of related cyclic compounds by a newly isolated
410 *Mycobacterium* sp. PH-06. Biodegradation **20:**511-519.
411 13. **Shen W, Chen H, Pan S.** 2008. Anaerobic biodegradation of 1,4-dioxane by sludge
412 enriched with iron-reducing microorganisms. Bioresour Technol **99:**2483-2487.
413 14. **Mahendra S, Alvarez-Cohen L.** 2005. *Pseudonocardia dioxanivorans* sp. nov., a novel
414 actinomycete that grows on 1,4-dioxane. Int J Syst Evol Microbiol **55:**593-598.
415 15. **Sei K, Kakinoki T, Inoue D, Soda S, Fujita M, Ike M.** 2010. Evaluation of the
416 biodegradation potential of 1,4-dioxane in river, soil and activated sludge samples.
417 Biodegradation **21:**585-591.
418 16. **Mahendra S, Petzold CJ, Baidoo EE, Keasling JD, Alvarez-Cohen L.** 2007.
419 Identification of the intermediates of in vivo oxidation of 1,4-dioxane by monooxygenase-
420 containing bacteria. Environ Sci Technol **41:**7330-7336.
421 17. **Grostern A, Sales CM, Zhuang WQ, Erbilgin O, Alvarez-Cohen L.** 2012. Glyoxylate
422 metabolism is a key feature of the metabolic degradation of 1,4-dioxane by
423 *Pseudonocardia dioxanivorans* strain CB1190. Appl Environ Microbiol **78:**3298-3308.
424 18. **Sales CM, Mahendra S, Grostern A, Parales RE, Goodwin LA, Woyke T, Nolan M,
425 Lapidus A, Chertkov O, Ovchinnikova G, Sczyrba A, Alvarez-Cohen L.** 2011.
426 Genome sequence of the 1,4-dioxane-degrading *Pseudonocardia dioxanivorans* strain
427 CB1190. J Bacteriol **193:**4549-4550.
428 19. **Daye KJ, Groff JC, Kirpekar AC, Mazumder R.** 2003. High efficiency degradation of
429 tetrahydrofuran (THF) using a membrane bioreactor: identification of THF-degrading
430 cultures of *Pseudonocardia* sp. strain M1 and *Rhodococcus ruber* isolate M2. J Ind
431 Microbiol Biotechnol **30:**705-714.
432 20. **Kampfer P, Kohlweyer U, Thiemer B, Andreesen JR.** 2006. *Pseudonocardia*
433 *tetrahydrofuranoxydans* sp nov. Int J Syst Evol Microbiol **56:**1535-1538.
434 21. **Kohlweyer U, Thiemer B, Schrader T, Andreesen JR.** 2000. Tetrahydrofuran
435 degradation by a newly isolated culture of *Pseudonocardia* sp. strain K1. FEMS
436 Microbiol Lett **186:**301-306.
437 22. **Thiemer B, Andreesen J, Schräder T.** 2003. Cloning and characterization of a gene
438 cluster involved in tetrahydrofuran degradation in *Pseudonocardia* sp. strain K1. Arch
439 Microbiol **179:**266-277.
440 23. **Masuda H, McClay K, Steffan R, Zylstra G.** 2012. Biodegradation of tetrahydrofuran
441 and 1,4-dioxane by soluble diiron monooxygenase in *Pseudonocardia* sp. strain ENV478.
442 J Mol Microbiol Biotechnol **22:**312-316.
443 24. **Yao Y, Lv Z, Min H, Jiao H.** 2009. Isolation, identification and characterization of a

AEM Accepts published online ahead of print

444 novel *Rhodococcus* sp. strain in biodegradation of tetrahydrofuran and its medium
445 optimization using sequential statistics-based experimental designs. Bioresour Technol
446 **100:**2762-2769.
447 25. **McLeod MP, Warren RL, Hsiao WW, Araki N, Myhre M, Fernandes C, Miyazawa**
448 **D, Wong W, Lillquist AL, Wang D, Dosanjh M, Hara H, Petrescu A, Morin RD,**
449 **Yang G, Stott JM, Schein JE, Shin H, Smailus D, Siddiqui AS, Marra MA, Jones SJ,**
450 **Holt R, Brinkman FS, Miyauchi K, Fukuda M, Davies JE, Mohn WW, Eltis LD.**
451 2006. The complete genome of *Rhodococcus* sp. RHA1 provides insights into a catabolic
452 powerhouse. Proc Natl Acad Sci U S A **103:**15582-15587.
453 26. **Johnson DR, Brodie EL, Hubbard AE, Andersen GL, Zinder SH, Alvarez-Cohen L.**
454 2008. Temporal transcriptomic microarray analysis of "*Dehalococcoides ethenogenes*"
455 strain 195 during the transition into stationary phase. Appl Environ Microbiol **74:**2864-
456 2872.
457 27. **Gentleman R.** 2005. Bioinformatics and computational biology solutions using R and
458 Bioconductor. Springer, New York.
459 28. **Gautier L, Cope L, Bolstad B, Irizarry R.** 2004. affy--analysis of Affymetrix GeneChip
460 data at the probe level. Bioinformatics **20:**307-315.
461 29. **Smyth GK.** 2004. Linear models and empirical bayes methods for assessing differential
462 expression in microarray experiments. Stat Appl Genet Mol Biol **3:**Article3.
463 30. **Benjamini Y, Hochberg Y.** 1995. Controlling the False Discovery Rate: A Practical and
464 Powerful Approach to Multiple Testing. J R Stat Soc Series B Stat Methodol **57:**289-300.
465 31. **Vandesompele J, De Preter K, Pattyn F, Poppe B, Van Roy N, De Paepe A,**
466 **Speleman F.** 2002. Accurate normalization of real-time quantitative RT-PCR data by
467 geometric averaging of multiple internal control genes. Genome Biol
468 **3:**research0034.0031-research0034.0011.
469 32. **Raymond David P.** 1987. New and versatile cloning vectors with kanamycin-resistance
470 marker. Gene **56.**
471 33. **Nakashima N, Tamura T.** 2004. Isolation and characterization of a rolling-circle-type
472 plasmid from *Rhodococcus erythropolis* and application of the plasmid to multiple-
473 recombinant-protein expression. Appl Environ Microbiol **70:**5557-5568.
474 34. **Sharp JO, Sales CM, LeBlanc JC, Liu J, Wood TK, Eltis LD, Mohn WW, Alvarez-**
475 **Cohen L.** 2007. An inducible propane monooxygenase is responsible for N-
476 Nitrosodimethylamine degradation by *Rhodococcus* sp. strain RHA1. Appl Environ
477 Microbiol **73:**6930-6938.
478 35. **Kaufman E, Nelson T, Fales H, Levin D.** 1988. Isolation and characterization of a
479 hydroxyacid-oxoacid transhydrogenase from rat kidney mitochondria. J Biol Chem
480 **263:**16872-16879.
481 36. **Bergmeyer H, Gawehn K, Klotzsch H, Krebs H, Williamson D.** 1967. Purification and
482 properties of crystalline 3-hydroxybutyrate dehydrogenase from *Rhodopseudomonas*
483 *spheroides*. Biochem J **102:**423-431.
484 37. **Söhling B, Gottschalk G.** 1996. Molecular analysis of the anaerobic succinate
485 degradation pathway in *Clostridium kluyveri*. J Bacteriol **178:**871-880.
486 38. **Mohr T, Stickney J, Diguiseppi B.** 2010. Environmental investigation and remediation :
487 1,4-dioxane and other solvent stabilizers. CRC Press, Boca Raton, FL.
488 39. **Sharp JO, Sales CM, LeBlanc J, Liu J, Wood TK, Eltis L, Mohn WW, Alvarez-**
489 **Cohen L.** 2007. An Inducible Propane Monooxygenase is Responsible for N-
490 nitrosodimethylamine Degradation by Rhodococcus sp. RHA1. Applied and

AEM Accepts published online ahead of print

491 Environmental Microbiology **73:**9.
492 40. **Kotani T, Yamamoto T, Yurimoto H, Sakai Y, Kato N.** 2003. Propane monooxygenase
493 and NAD+-dependent secondary alcohol dehydrogenase in propane metabolism by
494 *Gordonia* sp. strain TY-5. J Bacteriol **185:**7120-7128.
495 41. **Furuya T, Hayashi M, Semba H, Kino K.** 2012. The mycobacterial binuclear iron
496 monooxygenases require a specific chaperonin-like protein for functional expression in a
497 heterologous host. The FEBS journal **208:**817-826.
498 42. **Colby J, Dalton H, Whittenbury R.** 1975. An improved assay for bacterial methane
499 mono-oxygenase: some properties of the enzyme from *Methylomonas methanica*.
500 Biochem J **151:**459-462.
501 43. **Stirling DI, Dalton H.** 1977. Effect of metal-binding and other compounds on methane
502 oxidation by two strains of *Methylococcus capsulatus*. Arch Microbiol **114:**71-76.
503 44. **Prior SD, Dalton H.** 1985. Acetylene as a suicide substrate and active-site probe for
504 methane monooxygenase from *Methylococcus capsulatus* (Bath). FEMS Microbiol Lett
505 **29:**105-109.
506 45. **Hamamura N, Storfa RT, Semprini L, Arp DJ.** 1999. Diversity in butane
507 monooxygenases among butane-grown bacteria. Appl Environ Microbiol **65:**4586-4593.
508 46. **Sharp JO, Wood TK, Alvarez-Cohen L.** 2005. Aerobic biodegradation of N-
509 Nitrosodimethylamine (NDMA) by axenic bacterial strains. Biotechnol Bioeng **89:**608-
510 618.
511 47. **White GF, Russell NJ, Tidswell EC.** 1996. Bacterial scission of ether bonds. Microbiol
512 Rev **60:**216-232.
513
514

515 ## Figures and Tables

516 **FIG 1 THF and 1,4-dioxane degradation pathways.** Proposed reaction pathways for THF and
517 dioxane metabolism in CB1190, annotated with enzymes based on transcriptomic results in this
518 study. The THF pathway is adapted from the pathways proposed by Bernhardt and Diekmann (1),
519 Skinner *et al.* (7), and Thiemer *et al.* (22). The 1,4-dioxane pathway is adapted from Grostern *et*
520 *al*. (2012). The gene locus tags for the enzymes in the THF pathway are THF monooxygenase
521 *thmADBC* (Psed_6976 to Psed_6979), alcohol dehydrogenase (Psed_0131), hydroxyacid-oxoacid
522 transhydrogenase (Psed_6971), 4-hydroxybutyrate dehydrogenase (Psed_6970), succinate
523 semialdehyde dehydrogenase *sad* (Psed_6975), and aldehyde dehydrogenase *aldH* (Psed_6981).
524 The locus tags are the same for the dioxane pathway, except the secondary alcohol

525 dehydrogenase (Psed_0131, Psed_2070, Psed_4156, or Psed_6971) and the aldehyde

526 dehydrogenase (Psed_6971, Psed_6975, or Psed_6981)

527 **FIG 2 Functional activity of heterologous CB1190 THF MO expression clones.** (A) THF

528 removal by RHA1 containing plasmid pTip-CB1190-thfmo ■, the empty vector pTip-QC2

529 (control) □, and abiotic samples ○. (B) Removal of dioxane and accumulation of HEAA by

530 plasmid pTip-CB1190-thfmo clones, ■ (dioxane) and ▲ (HEAA); empty vector pTip-QC2

531 clones, □ (dioxane) and Δ (HEAA); and abiotic samples, ○ (dioxane) and ◊ (THF). Error bars

532 indicate standard deviations. All conditions were run in triplicate

533 **FIG 3 HEAA and dioxane degradation by CB1190.** (A) Disappearance of HEAA during

534 growth of CB1190 on HEAA as the sole carbon and energy source. Effect of acetylene exposure

535 on HEAA (B) and dioxane (C) degradation by CB1190. Acetylene-exposed cells ■, non-

536 acetylene exposed cells ○, and abiotic controls Δ were all performed in triplicate. Error bars

537 indicate standard deviations

538 **Table 1 Transcription of CB1190 genes proposed to be involved in THF metabolism**

AEM Accepts published online ahead of print

AEM Accepts published online ahead of print

539 **Table 1 Transcription of CB1190 genes proposed to be involved in THF metabolism**

Gene Locus Tag	Gene Name	Protein	log_2FC THF/Pyruvate	adjusted p-value	log_2FC Succinate/Pyruvate	adjusted p-value
Psed_0131		Alcohol dehydrogenase GroES domain protein	1.92	2.23E-05	0.53	9.87E-02
Psed_6970		D-lactate dehydrogenase (cytochrome)	2.75	5.49E-05	-0.18	7.86E-01
Psed_6971		Hydroxyacid-oxoacid transhydrogenase	2.17	7.06E-05	0.47	2.65E-01
Psed_6972		GntR domain protein	1.65	1.26E-03	0.26	6.35E-01
Psed_6974		Ethyl tert-butyl ether degradation EthD	1.78	8.85E-07	0.94	2.42E-04
Psed_6975	*sad*	Betaine-aldehyde dehydrogenase	1.65	2.73E-07	0.73	4.01E-04
Psed_6977	*thmD*	Ferredoxin--NAD(+) reductase	2.47	2.42E-07	0.68	1.00E-02
Psed_6978	*thmB*	Methane/phenol/toluene hydroxylase	1.58	3.75E-07	0.51	5.01E-03
Psed_6979	*thmC*	Monooxygenase component MmoB/DmpM	2.21	6.61E-07	0.69	9.03E-03
Psed_6981	*aldH*	Aldehyde Dehydrogenase	3.38	1.67E-07	0.96	6.65E-03
Psed_6982		Mn2+/Fe2+ transporter, NRAMP family	3.45	4.75E-06	0.21	7.34E-01

540

AEM Accepts published online ahead of print

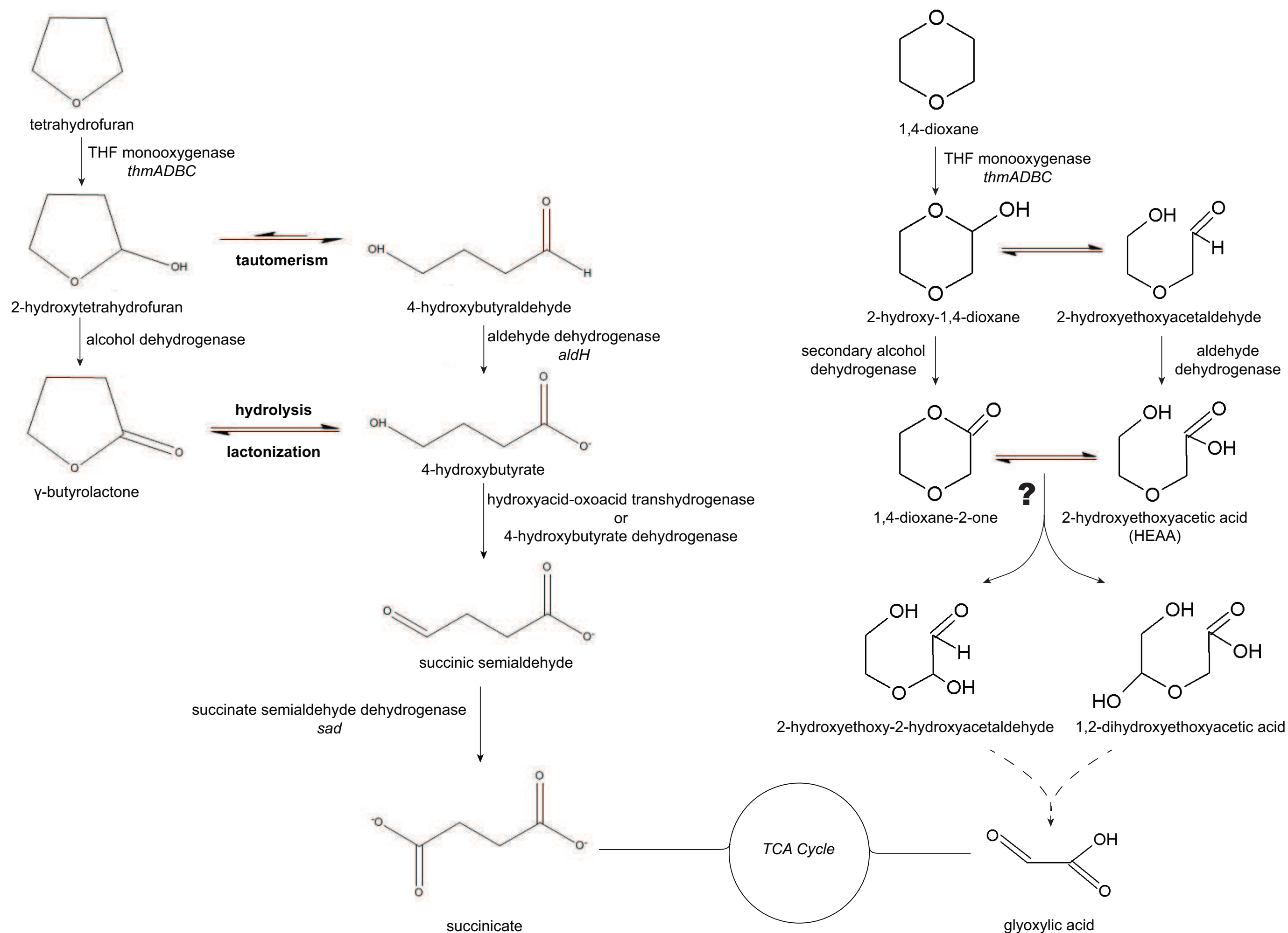

AEM Accepts published online ahead of print

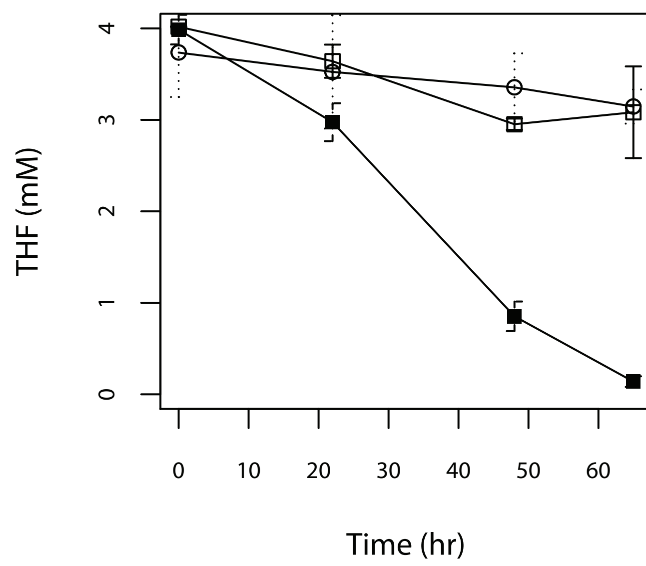

AEM Accepts published online ahead of print

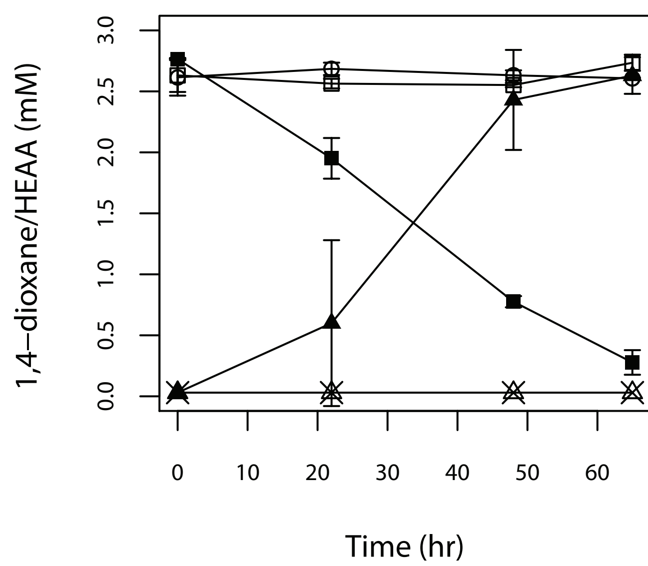

AEM Accepts published online ahead of print

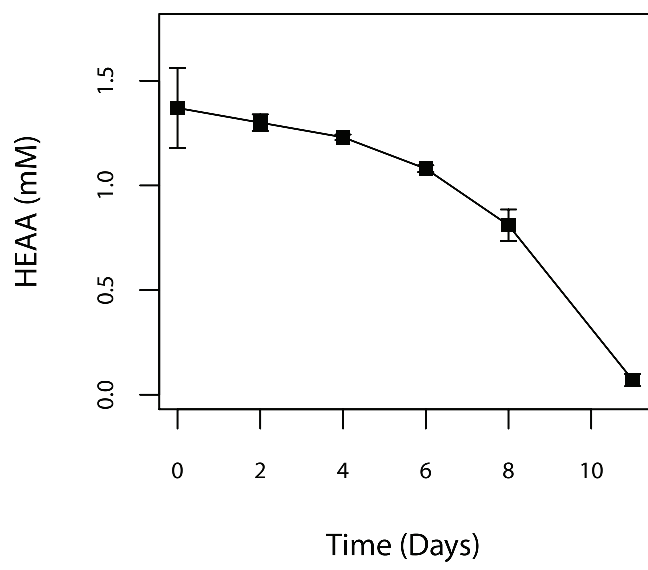

AEM Accepts published online ahead of print

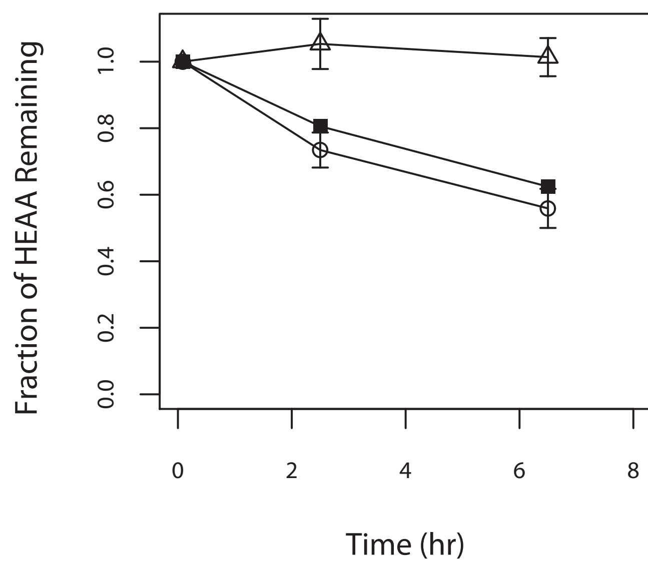

AEM Accepts published online ahead of print